PROCEEDINGS OF SCIENCE

Towards Understanding the Origin of Cosmic-Ray Positrons

Dimitrii Krasnopevtsev[†,*]

Massachusetts Institute of Technology, Cambridge, USA

E-mail: Dimitriy.Krasnopevtsev@cern.ch

Precision measurements of cosmic ray positrons are presented up to 1.4 TeV based on 3.4 million positrons collected by the Alpha Magnetic Spectrometer on the International Space Station. The positron flux exhibits complex energy dependence. Its distinctive properties are: (a) a significant excess starting from 24.2 GeV compared to the lower-energy, power-law trend; (b) a sharp drop-off above 268 GeV; (c) in the entire energy range the positron flux is well described by the sum of a term associated with the positrons produced in the collision of cosmic rays, which dominates at low energies, and a new source term of positrons, which dominates at high energies; and (d) a finite energy cutoff of the source term at 887 GeV. These experimental data on cosmic ray positrons show that, at high energies, they predominantly originate either from dark matter annihilation or from new astrophysical sources.

41st International Conference on High Energy physics - ICHEP2022
6-13 July, 2022
Bologna, Italy

*Speaker
†On Behalf of the AMS Collaboration.

PoS(ICHEP2022)281

1. Introduction

Studies of light cosmic ray antimatter species, such as positrons, are crucial for the understanding of new phenomena in the cosmos, since the yields of these particles from cosmic ray collisions with the interstellar medium are small. There has been widespread interests and various explanations [1] of the observed excess of high energy positrons [2]. Most of these explanations differ in their predictions for the behaviour of cosmic ray positrons at high energies.

In this proceeding precision measurements of primary cosmic-ray positrons up to 1.4 TeV with the Alpha Magnetic Spectrometer (AMS) on the International Space Station are presented. The measurements are based on 3.4 million positron events collected by the AMS during the first 10 years of operation started in May 2011. The AMS detector is described in detail in Ref. [3] and references therein. The key detector elements used for this analysis to efficiently separate positron candidates from background are the transition radiation detector, the time of flight counters, the silicon tracker, the permanent magnet, and the electromagnetic calorimeter. Template fit methods are used to determine the number of positrons in each energy bin. For the analysis details please refer to AMS publication in PRL [2].

2. Results.

The AMS positron spectrum is presented in Fig. 1. The spectrum is defined as the flux Φ_{e^+} scaled by $\tilde{E}^3$, where $\tilde{E}$ is the spectrally weighted mean energy [4]. In this and the subsequent figures, the error bars correspond to the quadratic sum of statistical and systematic errors. As seen, the positron spectrum exhibits complex energy dependence. At low energies, the spectrum varies due to solar modulation. At higher energies, the vertical colour bands indicate the energy ranges corresponding to changing behaviour of the spectrum: fattening, rising, and falling.

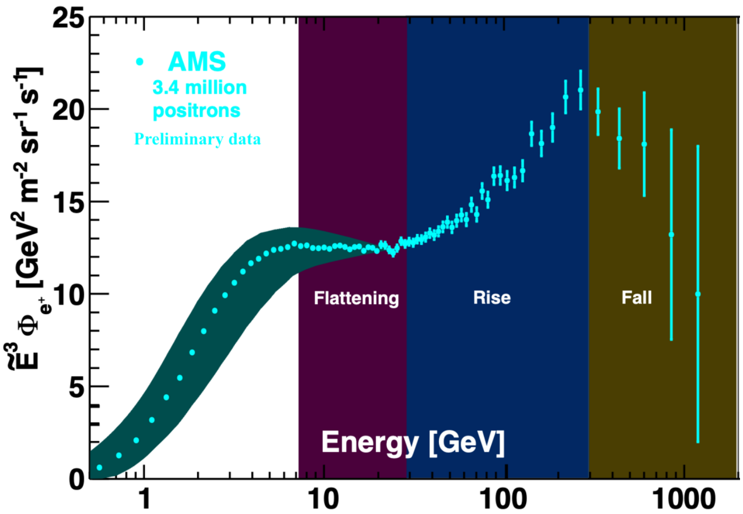

Figure 1: The AMS positron spectrum, $\tilde{E}^3\Phi_{e^+}$ (blue data points) is shown as a function of energy. The time variation of the flux at low energies due to solar modulation is indicated by the teal band. A preliminary data is shown here and on following plots (please refer to the upcoming AMS PRL publication).

PoS(ICHEP2022)281

To examine a changing behaviour of the positron spectrum a power law approximation with spectral index γ below a characteristic transition energy E_0 and $\gamma + \Delta\gamma$ above E_0 was used:

$$\Phi_{e^+}(E) = \begin{cases} CE^{\gamma}, & E \leq E_0; \\ CE^{\gamma}(E/E_0)^{\Delta\gamma}, & E > E_0. \end{cases} \tag{1}$$

The result of the fits of the Eq. 1 is shown on Fig. 2. It was found: (a) a significant excess starting from 24.2±1.1 GeV compared to the lower-energy, power-law trend; (b) a sharp drop-off above 268^{+91}_{-64} GeV. The significance of the increase above 24.2 GeV is established at more than 7 σ, while the significance of the drop-off above 268 GeV is established at 4.8 σ.

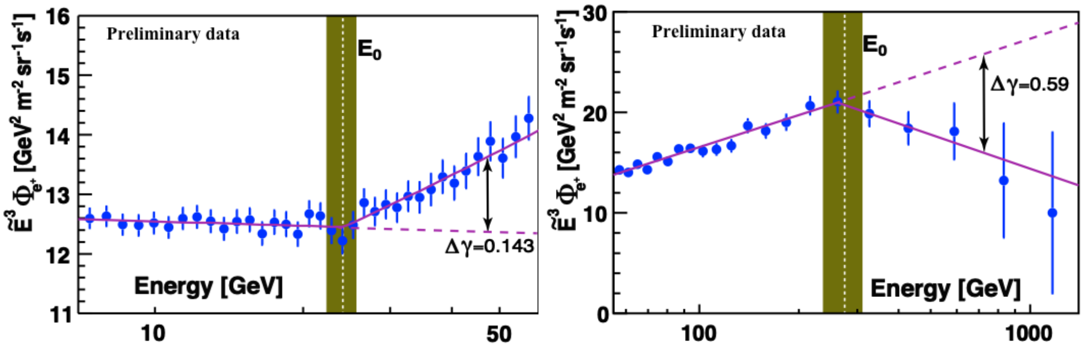

Figure 2: Fits of the Eq. 1 to the positron flux in the energy ranges [7.10 – 55.58] and [55.58 – 1400] GeV are represented by the solid violet lines in left and right graphs correspondingly. The vertical dashed lines correspond to the values of the energy E_0 where the changes of the spectral index occur and olive bands correspond to their errors. The dashed violet lines are the extrapolations of the power law from below E_0 into the higher energy regions. $\Delta\gamma$ is the magnitude of the spectral index change.

GALPROP model [5] is widely regarded as a standard framework for prediction of fluxes of secondary positrons based on the data from accelerator experiments and from cosmic-ray studies. Figure 3 shows comparison of the GALPROP prediction and AMS positron data. The model prediction below 3 GeV is in good agreement with data, followed by a peak in the spectrum of secondary positrons below 10 GeV and then a steady decrease with increasing energy. At high energies AMS positron flux is not consistent with the exclusive secondary production of positrons in collisions of cosmic rays. It suggests an extra source for primary cosmic ray positrons.

The accuracy of the AMS data allows for a detailed study of the properties of the new source of positrons. Figure 4 shows the analysis of the positron spectrum using a model, in which the flux is parametrized as the sum of two power law terms:

$$\Phi_{e^+}(E) = \frac{E^2}{\hat{E}^2}[C_1(\hat{E}/E_1)^{\gamma_1} + C_2(\hat{E}/E_2)^{\gamma_2}\exp(-\hat{E}/E_s)]. \tag{2}$$

The first term is related to the positrons production in the collisions of ordinary cosmic rays with the interstellar medium. It is characterized by a normalization factor C_1 and a spectral index γ_1. The second term has an exponential cutoff, which describes the high energy part of the flux dominated by a source. It is characterized by a cutoff energy E_s, a normalization factor C_s, and a

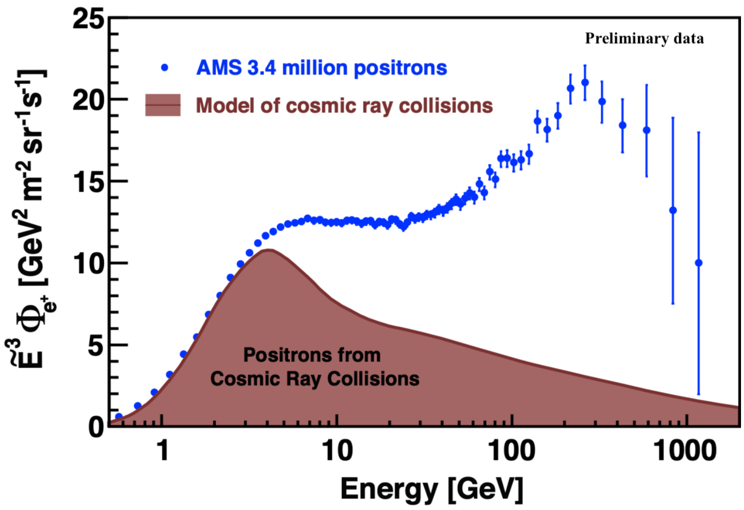

Figure 3: Comparison of the AMS data (blue data points) with a GALPROP model prediction [5] for the secondary positron spectrum (brown shaded area).

spectral index γ_2. The force-field approximation [6] is used to account for solar modulation effect. A detailed description of the parameters and their fitted values can be found in Ref. [2].

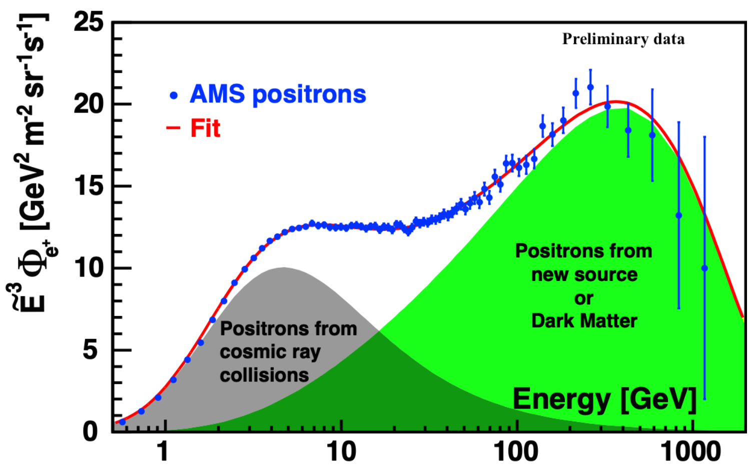

Figure 4: The fit of Eq. 2 (red line) to the positron flux in the energy range [0.5 - 1400] GeV. The blue data points represent the measured positron spectrum. The source term contribution is represented by the green area, and the term related to the secondary positron production is shown by the grey area.

As seen in Fig. 4, the first term dominates at low energies and then gradually vanishes with increasing energy. The contribution of the source term leads to the observed excess of the positron flux above 24.2 GeV. The drop-off of the flux above 268 GeV is very well described by the sharp exponential cutoff of the source term. The fitted value of the inverse cutoff energy, $1/E_s$ from Eq. 2, corresponds to $E_s = 887^{+313}_{-183}$ GeV. The significance of the source term energy cutoff is established at 4.5 σ. The experimental data on cosmic ray positrons show that, at high energies, positrons predominantly originate whether from dark matter annihilation or from other astrophysical sources.

Astrophysical point sources, like pulsars, will imprint a higher anisotropy on the arrival directions of energetic positrons than a smooth dark matter halo. Current AMS measurements show that the incoming directions of positrons are consistent with isotropic distribution [3]. In addition, cosmic-ray antiproton flux measured by AMS is an important observation to understand the origin of cosmic-ray antimatters. Surprisingly, the AMS measurements show that the positron spectrum and the antiproton spectrum have strikingly similar behavior at high energies [3]. It suggests a possible common source of high energy positrons and antiprotons. Antiprotons are not produced by pulsars and can't account for the observed hard spectrum of cosmic ray antiprotons.

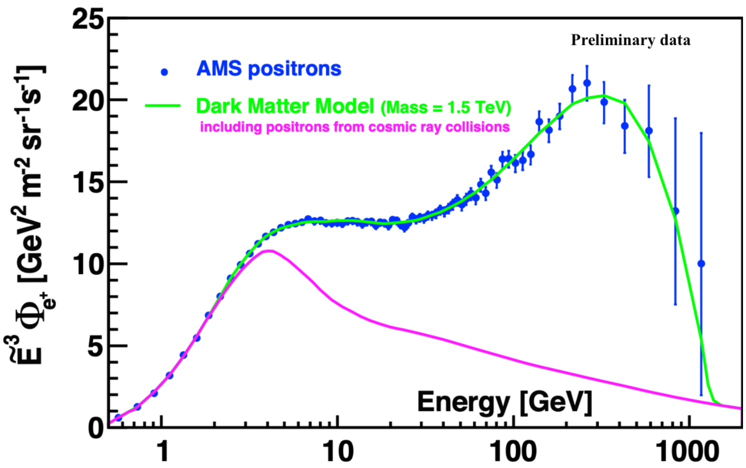

Figure 5: Comparison of the AMS data (blue points) with predictions of dark matter model based on Ref. [7, 8] with M_χ = 1.5 TeV (green curve). Contibution from cosmic ray collisions Ref. [5] is shown by pink curve.

High energy positron may originate from dark matter annihilation. As an example, Fig. 5 shows the comparison of AMS data with a dark matter model based on Ref. [7, 8] with M_χ = 1.5 TeV together with the contribution from cosmic ray collisions [5]. This good agreement needs to be verified with more statistics at high energies.

3. Prospects.

The study of the rate at which the positron spectrum falls beyond the turning point continues. Figure 6 shows the projected results for the positron spectrum from AMS through 2030. This projection includes future AMS detector upgrade in the incoming years. This upgrade will add a layer of silicon tracker on top of the AMS, increasing its acceptance by 300%. With the increase in statistics, the measurements will be extended up to 2 TeV, enabling to determine the origin of the positron excess, i.e. to distinguish the dark matter origin of the excess from other new astrophysical explanations, such as high energy positrons originating from pulsars.

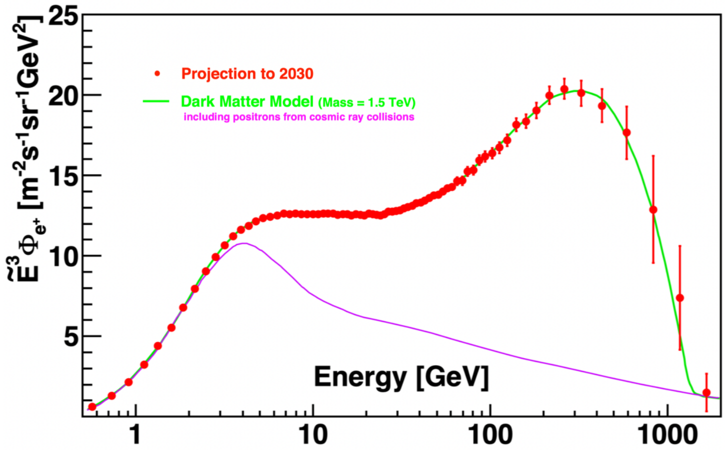

Figure 6: Projected AMS positron spectrum to 2030 (red data points). The results are compared with the same predictions as in Fig. 5.

Acknowledgments

This work has been supported by persons and institutions acknowledged in [2, 3].

References

[1] See, for example, M.S. Turner and F. Wilczek, Phys. Rev. D **42**, 1001 (1990); J. Ellis, AIP Conf. Proc. **516**, 21 (2000); M. Cirelli, R. Franceschini, and A. Strumia, Nucl. Phys. B **800**, 204 (2008); P. Blasi, Phys. Rev. Lett. **103**, 051104 (2009); T. Linden and S. Profumo, Astrophys. J. **772**, 18 (2013); P. Mertsch, A. Vittino, S. Sarkar, Phys. Rev. D **104**, 103029 (2021); R. Cowsik, B. Burch, and T. Madziwa-Nussinov, Astrophys. J. **786**, 124 (2014); M. Di Mauro, M.W. Winkler, Phys. Rev. D **103**, 123005 (2021).

[2] M. Aguilar *et al.*, Phys. Rev. Lett. **122**, 041102 (2019).

[3] M. Aguilar *et al.*, Phys. Rep. **894** (2021).

[4] G.D. Lafferty and T.R. Wyatt, NIM A **355**, 541 (1995).

[5] I.V. Moskalenko and A.W. Strong, Astrophys. J. **493**, 694 (1998).

[6] L. Gleeson, W. Axford, Astrophys. J. **154**, 1011 (1968).

[7] J. Kopp, Phys. Rev. D **88**, 076013 (2013).

[8] M. Cirelli *et al.*, J. Cosmol. Astropart. Phys. **03**, 051 (2011).